THE JOURNAL OF BIOLOGICAL CHEMISTRY VOL. 286, NO. 19, pp. 16807–16813, May 13, 2011

Modulation of Nucleotide Specificity of Thermophilic F_oF_1-ATP Synthase by ε-Subunit[S]

Received for publication, December 6, 2010, and in revised form, March 18, 2011 Published, JBC Papers in Press, March 23, 2011, DOI 10.1074/jbc.M110.209965

Toshiharu Suzuki[‡], Chiaki Wakabayashi[‡], Kazumi Tanaka[‡], Boris A. Feniouk[‡], and Masasuke Yoshida[‡§1]

From the [‡]ATP Synthesis Regulation Project, International Research Project (ICORP), Japan Science and Technology Corporation, Aomi 2-41, Tokyo 135-0064 and the [§]Department of Molecular Bioscience, Kyoto Sangyo University, Kamigamo, Kyoto 603-8555, Japan

The C-terminal two α-helices of the ε-subunit of thermophilic *Bacillus* F_oF_1-ATP synthase (TF_oF_1) adopt two conformations: an extended long arm ("up-state") and a retracted hairpin ("down-state"). As ATP becomes poor, ε changes the conformation from the down-state to the up-state and suppresses further ATP hydrolysis. Using TF_oF_1 expressed in *Escherichia coli*, we compared TF_oF_1 with up- and down-state ε in the NTP (ATP, GTP, UTP, and CTP) synthesis reactions. TF_oF_1 with the up-state ε was achieved by inclusion of hexokinase in the assay and TF_oF_1 with the down-state ε was represented by εΔc-TF_oF_1, in which ε lacks C-terminal helices and hence cannot adopt the up-state under any conditions. The results indicate that TF_oF_1 with the down-state ε synthesizes GTP at the same rate of ATP, whereas TF_oF_1 with the up-state ε synthesizes GTP at a half-rate. Though rates are slow, TF_oF_1 with the down-state ε even catalyzes UTP and CTP synthesis. Authentic TF_oF_1 from *Bacillus* cells also synthesizes ATP and GTP at the same rate in the presence of adenosine 5′-(β,γ-imino)triphosphate (AMP-PNP), an ATP analogue that has been known to stabilize the down-state. NTP hydrolysis and NTP-driven proton pumping activity of εΔc-TF_oF_1 suggests similar modulation of nucleotide specificity in NTP hydrolysis. Thus, depending on its conformation, ε-subunit modulates substrate specificity of TF_oF_1.

F_oF_1-ATP synthase (F_oF_1)[2] is ubiquitously found in membranes of bacteria, chloroplast, and mitochondria and synthesizes ATP by the energy of proton flow driven by the proton motive force. F_oF_1 also is able to catalyze the reverse reaction, ATP hydrolysis-driven proton pumping, which actually occurs in some cases and conditions. F_oF_1 is a motor enzyme composed of two rotary motors, membrane integral F_o, which converts the proton motive force into rotation, and water-soluble F_1, which converts the rotation into synthesis of ATP (1–10). F_1 has a subunit composition of $\alpha_3\beta_3\gamma\delta\epsilon$ and acts as ATPase when isolated. It has been known for the typical bacterial enzymes from thermophilic *Bacillus* PS3 (TF_oF_1) and *Escherichia coli*, that the smallest subunits of F_1, ε acts as an endogenous inhibitor of ATPase activity under some conditions (11–14). It is a 15-kDa protein composed of an N-terminal β-sandwich (~80 residues) and C-terminal α-helical (~50 residues) domains (15, 16). Two α-helices in the C-terminal domain undergo large conformational transition between the "up-state," in which the helices are extended as a long arm, and the C terminus reaches near the catalytic sites inside the $\alpha_3\beta_3$-ring, and the "down-state," in which the helices are retracted as a hairpin beside a globular domain of the γ-subunit (17–19). When ε is in the up-state, ATP hydrolysis is suppressed and transition to the down-state accompanies activation (20–22). The transition is induced by ATP (but not ADP) binding to F_1, and then the down-state is further stabilized by binding of ATP directly to ε (21, 23, 24). Consequently, ε favors the up-state in the absence of ATP even when high concentration of ADP is present, and it undergoes the transition to the down-state as ATP concentration raises. Apparent binding affinities of ATP (K_d) to cause the transition is 140 μM for TF_oF_1 at 59 °C, a physiological temperature of *Bacillus* PS3 (25). These values obviously are lower than the normal cellular ATP concentration of bacteria (~3 mM in *E. coli*) (26). Therefore, the function of C-terminal helices is assumed as "emergency brake" to prevent ATP hydrolysis, which works only when cellular ATP concentration decreased drastically under severely starving conditions (25, 27).

These contentions have been deduced mostly from analysis of ATP hydrolysis, and here, we studied the effect of conformational state of ε on ATP synthesis. As we have shown previously (20, 21), ε in TF_1 is predominantly in the up-state when ATP in the solution is eliminated by hexokinase. As a control mimicking TF_oF_1 with the down-state ε, we used a mutant εΔc-TF_oF_1, in which ε lacks C-terminal helices (27–30). Comparison of nucleotide specificity of wild-type TF_oF_1 (WT-TF_oF_1) and εΔc-TF_oF_1 in NTP (ATP, GTP, UTP, or CTP) synthesis reactions in the presence of hexokinase suggests that, when ε adopts the up-state conformation, TF_oF_1 gains higher nucleotide specificity to ATP. Results of NTP-driven proton pumping by εΔc-TF_oF_1 and NTP synthesis in the presence of adenosine 5′-(β,γ-imino)triphosphate (AMP-PNP) by TF_oF_1 are interpreted consistently by the above contention.

EXPERIMENTAL PROCEDURES

Preparation of Inverted Membrane Vesicles—In this study, WT- and εΔc-TF_oF_1 were expressed from plasmids pTR19-ASDS (31) and pTR19-ASDS-εΔc (29). The plasmids were introduced, respectively, into an F_oF_1-deficient *E. coli* strain,

[S] The on-line version of this article (available at http://www.jbc.org) contains supplemental Fig. S1.

[1] To whom correspondence should be addressed. E-mail: masasuke.yoshida@cc.kyoto-su.ac.jp.

[2] The abbreviations used are: F_oF_1, F_oF_1-ATP synthase; AMP-PNP, adenosine 5′-(β,γ-imino)triphosphate; CDTA, 1,2-cyclohexanediaminetetra-acetic acid; FCCP, carbonyl cyanide *p*-trifluoromethoxyphenylhydrazone; TF_oF_1, F_oF_1-ATP synthase from thermophilic *Bacillus* PS3; NTP, four kinds nucleotide triphosphates (ATP, GTP, UTP, CTP); NDP, four kinds nucleotide diphosphates (ADP, GDP, UDP, CDP); IMV, inverted membrane vesicle.

DK8 (bglR, thi-1, rel-1, HFrPO1, Δ(*uncB-uncC*), ilv:Tn10) (31). Cultivation of the recombinant strains and preparation of inverted membrane vesicles (IMVs) were performed as described (31). ATP hydrolysis activities of IMV containing WT- and ϵΔc-TF_oF_1 were inhibited efficiently (>80%) by dicyclohexylcarbodiimide. IMV was also prepared by the same procedures from thermophilic *Bacillus* PS3 cells that were cultured as described (33).

NTP Synthesis Assay with HPLC—NTP synthesis activity of IMV was measured with HPLC using an anion-exchange column, Super-Q 5PW (TOSOH Corp.). The column was equilibrated with 300 mM potassium phosphate buffer (pH 7.5) containing 10 mM CDTA at a flow rate of 1 ml/min. The NTP synthesis reaction was performed in 50 mM potassium phosphate buffer (pH 7.5) containing 5 mM $MgCl_2$, 15 μM adenosine-penta-5′-phosphate, 0.3 mM NDP, and IMV (72 μg proteins/ml). After incubation of the assay mixture for 2 min at 45 °C, 5 mM sodium succinate was added to initiate synthesis reaction. After the reaction (500 s), 10 mM CDTA was added to terminate the reaction. It was confirmed that 10 mM CTDA completely stopped synthesis and hydrolysis reactions (data not shown). The reaction mixtures were applied to a centrifugal concentrator (100 kDa, AmiconUltra) to remove IMV. Then, the pass-through fraction was applied to the column. Elution was monitored with absorbance at 260 nm. Separately, several concentrations of NTP and NDP were applied to the column to obtain the calibration curves by which peak areas were converted into nucleotide amount.

NTP Synthesis Assay with NDP-regenerating System—NTP synthesis activity of IMV was monitored in real time with an NDP-regenerating system at 45 °C in 25 mM potassium phosphate buffer (pH 7.5) containing 5 mM $MgCl_2$, 15 μM P^1,P^5-di(adenosine-5′)-pentaphosphate, 200 units/ml thermophilic hexokinase (TOYOBO) that can use NTP as a substrate, 25 units/ml thermophilic glucose-6-phosphate dehydrogenase (TOYOBO, Japan), 10 mM D-glucose, 0.5 mM NADP, IMV (72 μg proteins/ml), and 0.3 mM NDP. After preincubation of the assay mixture for 2 min at 45 °C, 5 mM sodium succinate was added to the mixture to generate electrochemical potentials of protons by the *E. coli* respiratory chain. At the end of the measurements, 1 μg/ml FCCP was supplemented to the reaction mixture to dissipate the potential and to know the slope of the base-line. NTP synthesis activity was calculated from the change in A_{340} during the period of 100 to 300 s after the succinate addition, using a molar absorbance coefficient of NADPH, 6220 A/M^{-1} cm^{-1}. The activity that synthesized one μmol of ATP per min was defined as one unit. Activities of synthesis of other NTPs, GTP, UTP, or CTP, were determined by introducing GDP, UDP, or CDP to the reaction mixture instead of ADP. The reaction mixture contained excess amount of hexokinase that converted NTPs to NDPs during the synthesis reactions. Judged from HPLC analysis, contamination of ATP in the ADP and AMP-PNP used in the experiments was <0.1%.

ATP Synthesis Assay with Luciferase—ATP synthesis in the presence of GTP, UTP, and CTP was measured by firefly luciferase that uses only ATP to emit luminescence (32). To avoid a large accumulation of ATP that could cause the conformational transition of ϵ-subunit, the lowest possible amount of IMV was used. Because of the heat-unstable nature of luciferase, reaction was performed at 37 °C. Reaction mixture contained 20 mM potassium phosphate (pH 7.5), IMV (3 μg proteins/ml), 5 mM $MgCl_2$, 0.3 mM ADP, 15 μM P^1,P^5-di(adenosine-5′)-pentaphosphate, and 1/10 volumes of the CLSII solution containing luciferin/luciferase (ATP bioluminescence assay kit, Roche Applied Science). The synthesis reaction was initiated by addition of 5 mM sodium succinate, and synthesis of ATP was monitored with the luminescence at 37 °C. At the end of each measurement, 1.7 μM ATP was added to the assay mixture several times to calibrate the luminescence intensity into ATP concentration. To view the effects of other NTPs (GTP, UTP, and CTP) and AMP-PNP on the activity, some or all of these components were supplemented to the reaction mixture at the final concentrations of 0.3 mM prior to the reaction. No significant luminescence was observed before addition of sodium succinate due to high specificity of luciferase toward ATP.

FRET Measurement—The conformational state of ϵ-subunit in TF_oF_1 was analyzed by FRET measurement 45 °C as described previously (25). Briefly, IMV containing TF_oF_1 labeled by fluorescent dyes (a donor Cy3 at the N terminus of the γ-subunit and an acceptor Cy5 at the C terminus of the ϵ-subunit) was prepared and suspended in 50 mM HEPES/KOH buffer (pH 7.5), 100 mM KCl, 5 mM $MgCl_2$, 0.5 mg/ml pyruvate kinase, and 2.5 mM phosphoenolpyruvate. Various concentrations of ATP was added, and the degree of the transition (up-state to down-state) was assessed after 40 min of incubation at 45 °C from the donor fluorescence at 566 nm.

Other Analytical Methods—NTP-driven proton pumping was monitored by fluorescence quenching of 9-amino-6-chloro-2-methoxyacridine (excitation at 410 nm, emission at 480 nm) at 43 °C as described previously (31). NTPase activities were measured at 45 °C in 50 mM HEPES/KOH buffer (pH 7.5) containing IMV (10 μg proteins/ml), 100 mM KCl, 5 mM $MgCl_2$, 0.2 μg/ml FCCP, indicated concentration of NTP, and the NTP-regenerating system composed of 0.5 mg/ml pyruvate kinase (from rabbit muscle, Roche Applied Science), 0.2 mg/ml lactate dehydrogenase, 2.5 mM phosphoenolpyruvate, 0.2 mM NADH, and 2.5 mM KCN (31, 34). Average hydrolysis rates in a time period from 3 to 6 min after initiation of the reactions were obtained. The activity that hydrolyzed one μmol of NTP per min was defined as one unit. Protein concentrations were determined by the BCA Protein Assay kit from Pierce, with bovine serum albumin as a standard. All data shown in the present study were measured at least in triplicate. *Error bars* in figures represent the standard deviations. Molar absorbance coefficients of 15,400 (259 nm), 13,700 (253 nm), 10,000 (262 nm), and 9000 A/M^{-1} cm^{-1} (271 nm) were used for quantification of AT(D)P, GT(D)P, UT(D)P, and CT(D)P throughout this study.

RESULTS

NTP Synthesis by WT-TF_oF_1 and ϵΔc-TF_oF_1—NTP synthesis by wild-type *Bacillus* PS3 TF_oF_1 (WT-TF_oF_1) and its mutant ϵΔc-TF_oF_1 was compared. Under the assay conditions, ϵ in WT-TF_oF_1 should be in the up-state without added ATP (25),

and ϵΔc-TF_oF_1, which lacks the C-terminal two helices (Ile^{88}–Lys^{133}) of ϵ, is thought to act as the TF_oF_1 with ϵ in the down-state. They were expressed in *E. coli* cells, and the IMV prepared from these cells was used for NTP synthesis measurements. SDS-PAGE analysis confirmed that the content of ϵΔc-TF_oF_1 in IMV was almost the same as that of WT-TF_oF_1 as reported previously (30). Nucleotides were identified and quantified with anion-exchange HPLC. Retention time of ADP was different from those of other NDPs, and we confirmed the absence of detectable contamination of ADP in the GDP, UDP, and CDP used in the experiments (Fig. 1*A*). The reaction mixtures contained 0.3 mM of one of NDPs and IMV containing WT-TF_oF_1 or ϵΔc-TF_oF_1. The synthesis reactions were started by addition of succinate to the mixture to generate the proton motive force through oxidation by the *E. coli* respiratory chain. After incubation for 500 s at 45 °C, the reactions were terminated by addition of 10 mM CDTA, and nucleotides were analyzed with HPLC (Fig. 1*B*). Control samples supplemented with an uncoupler, FCCP, or with 10 mM CDTA from the beginning gave the background elution profiles with no net NTP synthesis. IMV prepared from F_oF_1-deficient *E. coli* (DK8) did not show net NTP synthesis (supplemental data). The amounts of synthesized NTP were obtained from net increase of the peak areas, and the synthesis activities were calculated (Fig. 1*C*). Both WT-TF_oF_1 and ϵΔc-TF_oF_1 had apparently the same activity of ATP synthesis. However, ϵΔc-TF_oF_1 had a 2-fold higher activity of GTP synthesis than WT-TF_oF_1. A small amount of UTP synthesis was observed for ϵΔc-TF_oF_1 but not for WT-TF_oF_1. Net synthesis of CTP was not detected both for WT-TF_oF_1 and ϵΔc-TF_oF_1.

NTP Synthesis in Presence of NDP-regenerating System—In the above HPLC experiments, the back reaction (NTP hydrolysis) and up-to-down transition of ϵ in WT-TF_oF_1 became possible as the synthesized NTP accumulated with time. To avoid this possibility, we next included hexokinase in the assay to convert NTP into NDP. As shown previously (20, 21), ϵ in TF_oF_1 predominantly adopts the up-state conformation in the presence of hexokinase. The hexokinase used in the experiments accepts any NTPs as a substrate, and the produced glucose 6-phosphate was monitored (35). The reaction was started by addition of succinate to the reaction mixture containing 1 mM NDP and IMV (Fig. 2*A*). NTP synthesis proceeded at a constant rate after a short initial lag (<30 s). The activity values and nucleotide specificity of NTP synthesis of WT-TF_oF_1 measured with NDP-regenerating system at 0.3 mM NDP were almost the same as those measured with HPLC; ATP synthesis (=100%) > GTP synthesis (40–50%) ≫ UTP and CTP synthesis (~3%) (Fig. 2*B*, *left panel*). For ϵΔc-TF_oF_1, the activity values of ATP, GTP, and UTP synthesis were >2-fold higher than those measured with HPLC. Furthermore, small but significant CTP synthesis was detected in the presence of NDP-regenerating system. It appeared that, different from WT-TF_oF_1, ϵΔc-TF_oF_1 catalyzed hydrolysis of the synthesized NTP during the synthesis reaction and prevention of the hydrolysis by NDP-regenerating system made the synthesis activity larger. Nucleotide specificity in NTP synthesis by ϵΔc-TF_oF_1 observed with NDP-regenerating system showed the trend similar to that observed with HPLC; ATP synthesis (100%) ≈ GTP synthesis >

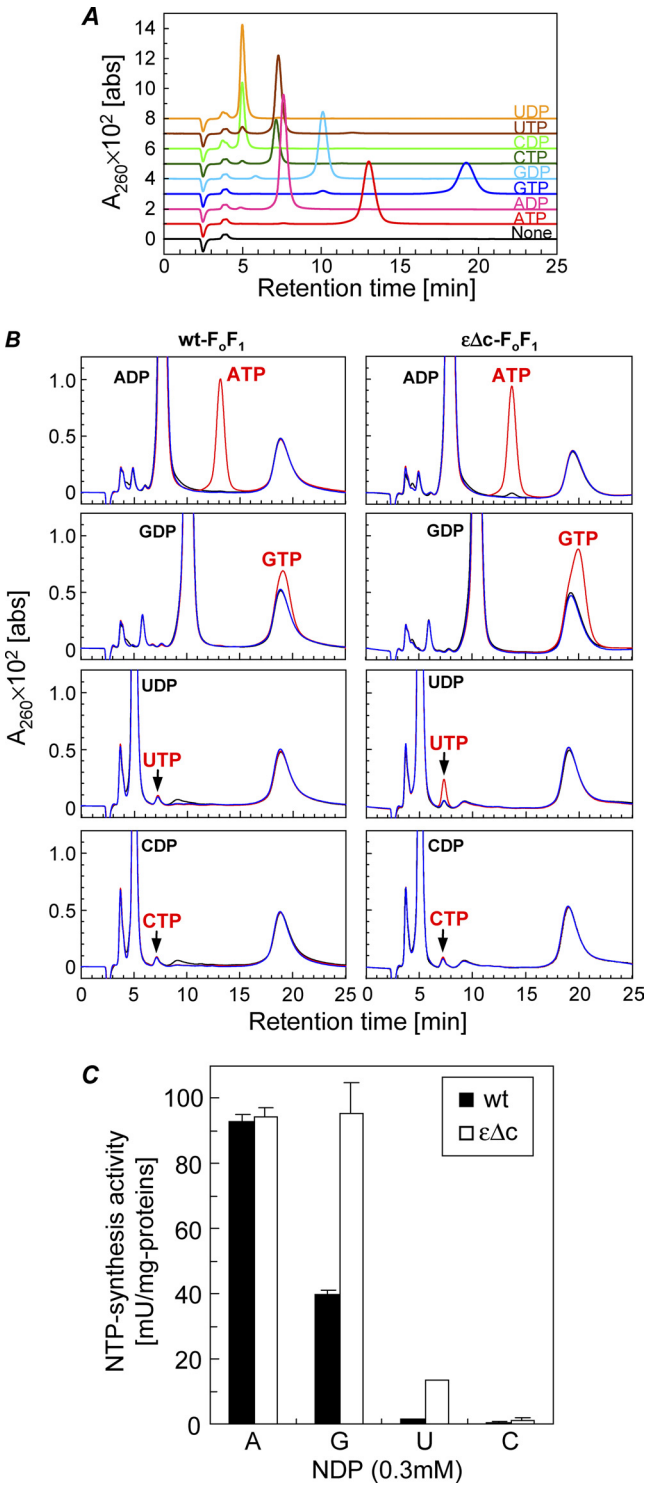

FIGURE 1. **Analysis of NTP synthesis with anion-exchange HPLC.** *A*, elution profiles of NTPs and NDPs. NT(D)P (8 nmol) in 10 mM CDTA was applied to the column. *B*, NTP synthesis by IMV prepared from *E. coli* cells expressing WT-TF_oF_1 (*left panels*) and ϵΔc-TF_oF_1 (*right panels*). The reaction mixture contained 0.3 mM NDP, 50 mM potassium phosphate, and IMV (72 μg proteins/ml). The reaction was initiated by addition of 5 mM sodium succinate. After incubation for 500 s at 45 °C, the reaction was terminated by addition of 10 mM CDTA, and the nucleotides in the reaction mixtures were analyzed with HPLC (*red trace*). In the control samples, 10 mM CDTA (*black traces*) or 1 μg/ml FCCP (*green traces*) were further included in the mixtures from the start of the reaction. The amount of synthesized NTP was determined from the net increase of the peak areas (*red* and *black*). *C*, comparison of NTP synthesis activities of WT-TF_oF_1 and ϵΔc-TF_oF_1. Detailed experimental conditions are as described under "Experimental Procedures." *abs*, absorbance.

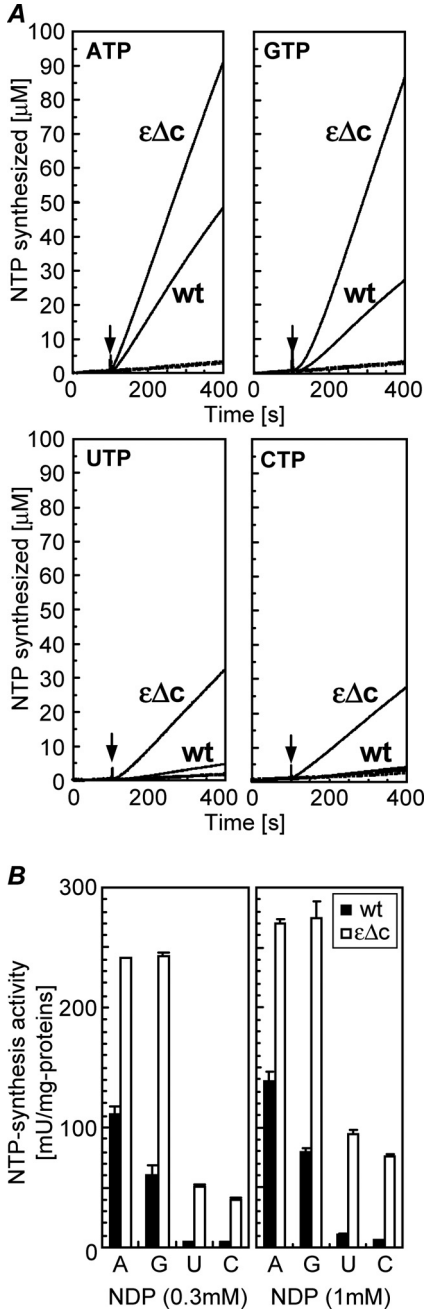

FIGURE 2. **NTP synthesis in the presence of NDP-regenerating system.** *A*, time courses of NTP-synthesis at 45 °C by IMV prepared from *E. coli* cells expressing WT- and ϵΔc-TF_oF_1. The reaction was initiated by addition of 5 mM sodium succinate into the reaction mixture containing 1 mM NDP, 25 mM potassium phosphate, IMV (72 μg proteins/ml), and the NDP-regenerating system (hexokinase, glucose-6-phosphate dehydrogenase, glucose, and NADP). NTP synthesis was monitored by NADPH production (A_{340}). Dotted lines show the time courses in the presence of 1 μg/ml FCCP. *B*, synthesis activities at 0.3 mM NDP (*left panel*) and 1 mM NDP (*right panel*). Experimental details are as described under "Experimental Procedures."

UTP synthesis (20%) > CTP synthesis (17%). The concentrations of substrate NDP in the above experiments were 0.3 mM and the difference between WT-TF_oF_1 and ϵΔc-TF_oF_1 potentially could be attributed to their different dependence on NDP concentration. However, it was not the case because essentially the same results were obtained at 1 mM NDP, indicating that the activities were already saturated as V_{max} at 0.3 mM NDP (Fig. 2*B*, *right panel*).

ATP and GTP Synthesis by WT-TF_oF_1 and ϵΔc-TF_oF_1 in Presence of AMP-PNP—It has been known that a nonhydrolyzable ATP analogue, AMP-PNP, can stabilize the down-state ϵ in F_1 (18, 20, 21). Taking advantage of the fact that AMP-PNP does not significantly inhibit ATP synthesis (36), we examined the effect of AMP-PNP on NTP synthesis by WT-TF_oF_1 and ϵΔc-TF_oF_1. ATP and GTP synthesis activities of ϵΔc-TF_oF_1 were, respectively, only slightly and not at all inhibited by AMP-PNP. In a sharp contrast, ATP and GTP synthesis activities of WT-TF_oF_1 were stimulated, respectively, nearly and >2-fold by AMP-PNP. ATP synthesis activity of WT-TF_oF_1 was stimulated as AMP-PNP concentration increased, and it reached the same level of that of ϵΔc-TF_oF_1 at 1 mM AMP-PNP (Fig. 3*A*). Similarly, GTP synthesis activity of WT-TF_oF_1 was stimulated by AMP-PNP, and the stimulated activity was almost the same as that of ϵΔc-TF_oF_1 at 2 mM AMP-PNP (Fig. 3*B*). AMP-PNP alone at 2 mM without ADP and GDP did not show any NTP synthesis activities, eliminating a possibility that contaminating ADP (or GDP) in AMP-PNP was responsible for the synthesis. Nucleotide specificity of the synthesis reaction by WT-TF_oF_1 was also changed by AMP-PNP. As seen in the activity of GTP-synthesis relative to ATP-synthesis (Fig. 3*C*), AMP-PNP stimulated GTP synthesis of WT-TF_oF_1 more markedly than ATP synthesis, apparently making nucleotide specificity of WT-TF_oF_1 similar to that of ϵΔc-TF_oF_1. Apparent dissociation constant of AMP-PNP ($K_{d(AMP\text{-}PNP)}$) in the stimulation of WT-TF_oF_1 was estimated to be 0.1∼0.3 mM. These results clearly show that WT-TF_oF_1 behaves as if it were ϵΔc-TF_oF_1 in the presence of sufficient concentration of AMP-PNP where ϵ in WT-TF_oF_1 adopts the down-state.

We also measured ATP synthesis reaction in the presence of 0.3 mM of GTP, UTP, and CTP. The synthesized ATP was assayed by luciferase that is highly specific to ATP. As seen (Fig. 3*D*), the presence of these nucleotides did not interfere with ATP synthesis by WT-TF_oF_1 and ϵΔc-TF_oF_1. Also, the effect of AMP-PNP on ATP synthesis was not influenced by these nucleotides. Therefore, GTP, UTP, and CTP have actually no effect on ATP synthesis; they do not compete with adenine nucleotides (ADP, ATP, and AMP-PNP) for catalytic or other modulatory nucleotide binding sites of TF_oF_1 under the conditions tested.

ATP and GTP Synthesis by Authentic TF_oF_1 of Bacillus Cells—Similar experiments were performed for IMV prepared from *Bacillus* PS3 cells. Measurement at 45 °C showed severalfold stimulation of ATP and GTP synthesis activities of authentic *Bacillus* PS3 TF_oF_1 by AMP-PNP (Fig. 4*A*) with an apparent $K_{d(AMP\text{-}PNP)}$ of 0.1∼0.3 mM. The thermostable auxiliary enzymes hexokinase and glucose-6-phosphate dehydrogenase enabled us to raise the assay temperature up to 58 °C, a physiological temperature of *Bacillus* PS3. At 58 °C, AMP-PNP stimulated ATP- and GTP-synthesis activities severalfold, but higher AMP-PNP concentration was needed to saturate the stimulatory effect (Fig. 4*B*). At either 45 or 58 °C, GTP synthesis activity increased more sharply than ATP synthesis as the AMP-PNP concentration rose, and both activities became almost equal at 2 mM (45 °C) or 3 mM (58 °C) AMP-PNP (Fig. 4*C*). Thus, AMP-PNP stimulates NTP synthesis activity of *Bacillus* PS3 TF_oF_1, either from recombinant *E. coli* cells or

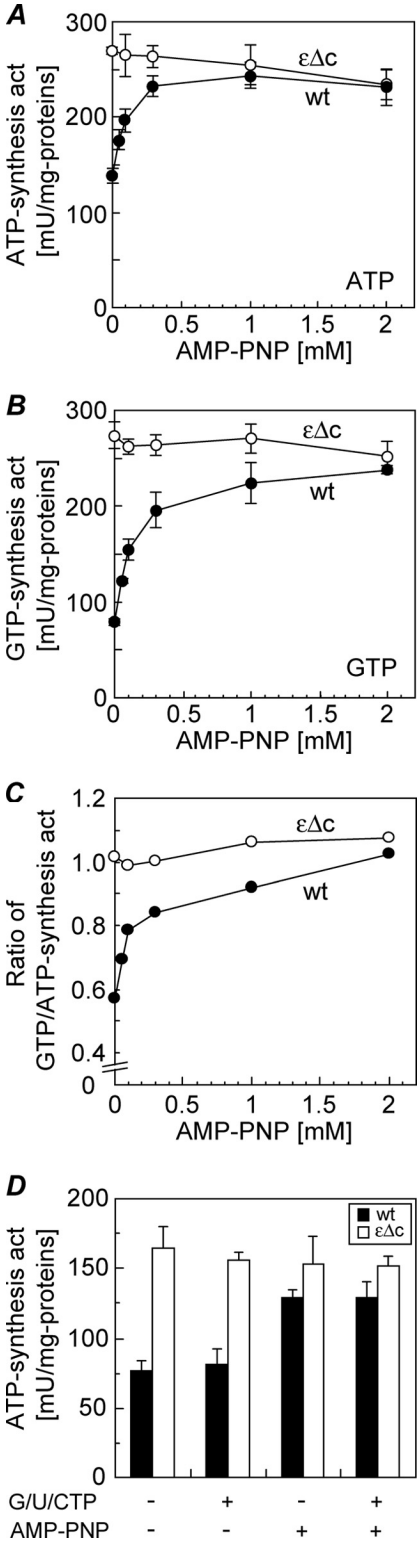

FIGURE 3. **Effect of AMP-PNP on ATP and GTP synthesis.** Effect of AMP-PNP on ATP synthesis activity (*A*) and GTP synthesis activities (*B*) of WT- and $\epsilon\Delta c$-TF_oF_1. The analytical conditions were the same as described in the legend to Fig. 2 except that AMP-PNP (0, 0.1, 0.3, 1, 2 mM and in some cases, 0.05 mM) was supplemented to the reaction mixture. *C*, effect of AMP-PNP on the specificity of substrate nucleotide of WT-TF_oF_1 and $\epsilon\Delta c$-TF_oF_1. Ratios of GTP to ATP synthesis activity were plotted against AMP-PNP concentration. *D*, effect of other NTPs (GTP, UTP, and CTP) on AMP-PNP-induced activation of ATP synthesis. ATP synthesis was monitored at 37 °C with luciferase. *G/U/CTP*, GTP+UTP+CTP (each 0.3 mM); *AMP-PNP*, 0.3 mM AMP-PNP; *mU*, milliunits. Experimental details are as described under "Experimental Procedures."

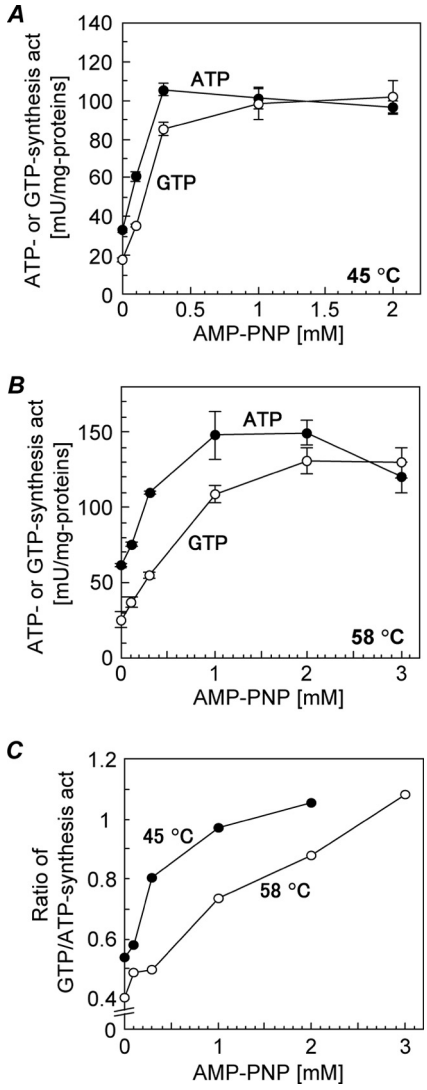

FIGURE 4. **Effect of AMP-PNP on ATP and GTP synthesis by authentic TF_oF_1.** *A*, analytical conditions were the same as in Fig. 3, except that IMV was prepared from thermophilic *Bacillus* PS3 cells. The reactions were carried out at 45 °C (*A*) or 58 °C (*B*). *C*, effect of AMP-PNP on the specificity of substrate nucleotide of authentic TF_oF_1. *mU*, milliunits.

Bacillus PS3 cells, with concomitant loss of strict nucleotide specificity.

NTP Hydrolysis and Proton Pumping by WT-TF_oF_1 and $\epsilon\Delta c$-TF_oF_1—We measured NTP hydrolysis activities (NTPase) of IMV containing WT-TF_oF_1 and $\epsilon\Delta c$-TF_oF_1. Activities were measured at 45 °C as NADH oxidation with auxiliary enzymes, pyruvate kinase and lactate dehydrogenase. Pyruvate kinase used in the experiments has a broad substrate specificity toward NTPs (34), and it keeps the initial NTP concentrations during reaction time by regenerating NTP from NDP. When ATPase activity at the same ATP concentration was compared between WT-TF_oF_1 and $\epsilon\Delta c$-TF_oF_1; both had similar activities at an ATP concentration >100 μM (Fig. 5*A*). Below 100 μM, however, ATPase activities of WT-TF_oF_1 became much smaller than those of $\epsilon\Delta c$-TF_oF_1 (Fig. 5*A*, *inset*). From the plot of activity of WT-TF_oF_1 relative to $\epsilon\Delta c$-TF_oF_1 as a function of ATP concentration, an ATP concentration that gave half-maximal activation of ATPase activity of WT-TF_oF_1 was estimated to be ~52

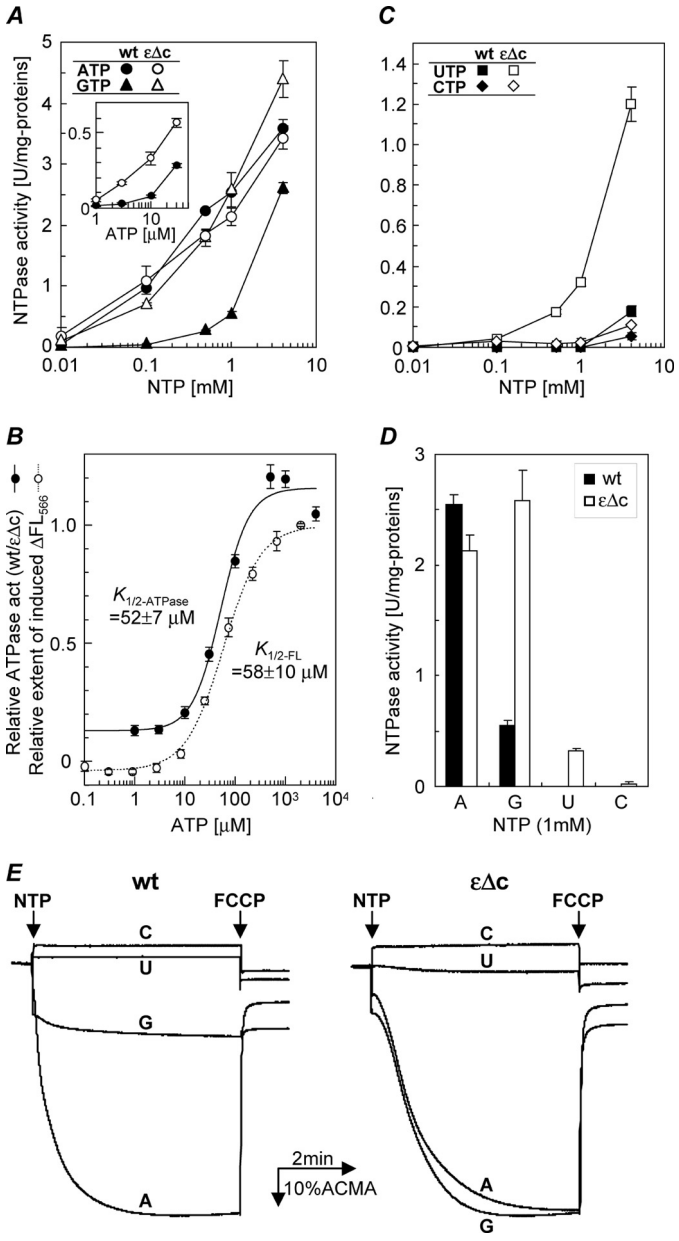

FIGURE 5. **Nucleotide specificity in hydrolysis and proton-pumping activities of WT-TF_oF_1 and ϵΔc-TF_oF_1.** *A*, activities of ATP hydrolysis and GTP hydrolysis of WT-TF_oF_1 and ϵΔc-TF_oF_1 at 45 °C. *B*, ATP-dependent activation of ATPase of WT-TF_oF_1 and the up-to-down conformational transition of ϵ probed by FRET change. *Closed circles*, ratios of ATPase activities (WT-TF_oF_1/ϵΔc-TF_oF_1) obtained from the data in *A*; *Open circles*, FRET represented by donor fluorescence intensity. High donor fluorescence reflected the down-state ϵ. *Lines* represent the best fit of the data points. *C*, activities of UTP hydrolysis and CTP hydrolysis of WT-TF_oF_1 and ϵΔc-TF_oF_1 at 45 °C. Note the different *y*-scale in *A* and *C*. *D*, comparison of the NTPase activities at 1 mM NTP. *E*, proton-pumping activity of WT-TF_oF_1 and ϵΔc-TF_oF_1 driven by 1 mM NTP. The proton pumping was monitored by the quenching of 9-amino-6-chloro-2-methoxyacridine fluorescence (*ACMA*) at 42 °C (10% quenching is shown in the figure). The reaction was initiated by adding 1 mM NTP and terminated by 1 μg/ml FCCP.

μM (Fig. 5*B*). We also measured the up-to-down transition of ϵ in WT-TF_oF_1 at 45 °C by change of FRET between dyes attached on the C terminus of ϵ and the N terminus of the γ-subunit (Fig. 5*B*) (25). At low ATP concentration, donor fluorescence was weak, and ϵ mostly adopted the up-state conformation. As ATP concentration increased, donor fluorescence increased reflecting increase in population of the down-state ϵ. An ATP concentration that gave half-maximum donor intensity was estimated to be ~58 μM. This value was smaller than the previous one (140 μM at 59 °C) because temperature was lower (25). Good coincidence between the two plots in Fig. 5*B* suggests that the up-to-down transition of ϵ in TF_oF_1 occurs at ~55 μM ATP accompanying activation of ATPase activity.

When GTP was a substrate, on the contrary, WT-TF_oF_1 had severalfold smaller activity than ATPase, whereas ϵΔc-TF_oF_1 hydrolyzed GTP at almost the same rate as ATP (Fig. 5*A*). Less strict nucleotide specificity of ϵΔc-TF_oF_1 was also observed in hydrolysis of UTP and CTP (Fig. 5*C*). WT-TF_oF_1 was almost unable to hydrolyze 1 mM UTP and CTP, but ϵΔc-TF_oF_1 hydrolyzed 1 mM UTP at a significant rate (~15% of ATPase) (Fig. 5*D*).

The nucleotide specificity of NTP-driven proton pumping activity of ϵΔc-TF_oF_1 was also compared with that of WT-TF_oF_1 (Fig. 5*E*). Upon addition of 1 mM nucleotide, a small, immediate shift of fluorescence level of 9-amino-6-chloro-2-methoxyacridine occurred due to direct interaction of 9-amino-6-chloro-2-methoxyacridine with nucleotide. The extent of the shift differed among nucleotide, with GTP as the largest. The shift was followed by relatively slow quenching of fluorescence that reflected acidification of the inside lumen of IMV. Proton pumping by WT-TF_oF_1 was driven efficiently by ATP, weakly by GTP, and not at all by UTP and CTP. In the case of ϵΔc-TF_oF_1, GTP was able to drive proton pumping as efficiently as ATP, and UTP showed a barely detectable pumping activity. From the results of ϵΔc-TF_oF_1, we can conclude that TF_oF_1 with down-state ϵ can utilize GTP as efficiently as ATP in hydrolysis reactions. As to WT-TF_oF_1, ATP hydrolysis and ATP-driven proton pumping should be catalyzed by WT-TF_oF_1 with the down-state ϵ because substrate ATP at 1 mM was present. On the contrary, conformational state of ϵ in 1 mM GTP should be a mixture of the up-state and the down-state (21), hampering the clear interpretation.

DISCUSSION

The ϵ-subunit has been long known as an intrinsic inhibitor of ATPase activity of F_1 and F_oF_1. Recent studies revealed that ϵ can adopt two conformations, and the up-state conformation is responsible for the inhibition. Furthermore, it was found that ATP can bind to and stabilizes the down-state ϵ in some bacteria (13). Here, we added another novel aspect of the functions of ϵ, that is, modulation of nucleotide specificity. Given that AMP-PNP would stabilize the down-state ϵ in TF_oF_1 under the experimental conditions, we can indicate that the native TF_oF_1 of *Bacillus* PS3 might also modulate nucleotide specificity by ϵ at a physiological temperature (Fig. 4). As well, ϵ is likely to modulates nucleotide specificity in ATP hydrolysis (Fig. 5).

From a structural aspect, higher nucleotide specificity of TF_oF_1 with the up-state ϵ is not surprising because the residues of the C-terminal region of ϵ can reach the location close to the catalytic site when C-terminal helices of the up-state ϵ are extended like a long arm into the inside of $\alpha_3\beta_3$ ring. We think it is likely because the introduced cysteines at βLys^{334} near the catalytic site and ϵGlu^{131} at the third position from the C ter-

minus can form a disulfide cross-link when ϵ is up-state in the absence of nucleotide.[3]

In the actively growing *E. coli* cell, cellular ATP concentration is in the range of ~3 mM (26) and concentrations of other three NTPs are estimated to be ~1.5 mM or 0.7–1.2 mM (GTP), and ~0.7 mM (UTP and CTP) (37, 38). Therefore, hydrolysis of the three NTPs by F_oF_1 with the down-state ϵ and, synthesis as well, can occur in the cell. Although its physiological significance is yet unclear, it is tempting to speculate that ϵ acts as an ATP-dependent switch that changes the mode of the enzyme operation. When the cell energy becomes poor and ATP concentration drops, TF_oF_1 would limit ATP and GTP consumption, and the synthesis activity is restricted to ATP.

In summary, our results suggest that the ϵ-subunit of F_oF_1-ATP synthase from a thermophilic *Bacillus* regulates not only magnitude of activity but also modulates specificity of substrate nucleotide both in synthesis and hydrolysis reactions, depending on its extended and retracted conformations.

Acknowledgments—We thank Drs. E. Saita, N. Taniguchi, and Y. Kato-Yamada for discussion.

REFERENCES

1. Yoshida, M., Muneyuki, E., and Hisabori, T. (2001) *Nat. Rev. Mol. Cell Biol.* **2,** 669–677
2. Boyer, P. D. (2002) *J. Biol. Chem.* **277,** 39045–39061
3. Senior, A. E., Nadanaciva, S., and Weber, J. (2002) *Biochim. Biophys. Acta* **1553,** 188–211
4. Kinosita, K., Jr., Adachi, K., and Itoh, H. (2004) *Annu. Rev. Biophys. Biomol. Struct.* **33,** 245–268
5. Nakamoto, R. K., Baylis Scanlon, J. A., and Al-Shawi, M. K. (2008) *Arch. Biochem. Biophys.* **476,** 43–50
6. Hong, S., and Pedersen, P. L. (2008) *Microbiol. Mol. Biol. Rev.* **72,** 590–641,
7. Junge, W., Sielaff, H., and Engelbrecht, S. (2009) *Nature* **459,** 364–370
8. Düser, M. G., Zarrabi, N., Cipriano, D. J., Ernst, S., Glick, G. D., Dunn, S. D., and Börsch, M. (2009) *EMBO J.* **28,** 2689–2696
9. von Ballmoos, C., Wiedenmann, A., and Dimroth, P. (2009) *Annu. Rev. Biochem.* **78,** 649–672
10. Nakanishi-Matsui, M., Sekiya, M., Nakamoto, R. K., and Futai, M. (2010) *Biochim. Biophys. Acta* **1797,** 1343–1352
11. Smith, J. B., and Sternweis, P. C. (1977) *Biochemistry* **16,** 306–311
12. Kato, Y., Matsui, T., Tanaka, N., Muneyuki, E., Hisabori, T., and Yoshida, M. (1997) *J. Biol. Chem.* **272,** 24906–24912
13. Feniouk, B. A., Suzuki, T., and Yoshida, M. (2006) *Biochim. Biophys. Acta* **1757,** 326–338
14. Feniouk, B. A., and Yoshida, M. (2008) *Results Probl. Cell Differ.* **45,** 279–308
15. Uhlin, U., Cox, G. B., and Guss, J. M. (1997) *Structure* **5,** 1219–1230
16. Wilkens, S., Dahlquist, F. W., McIntosh, L. P., Donaldson, L. W., and Capaldi, R. A. (1995) *Nat. Struct. Biol.* **2,** 961–967
17. Rodgers, A. J., and Wilce, M. C. (2000) *Nat. Struct. Biol.* **7,** 1051–1054
18. Kato-Yamada, Y., Yoshida, M., and Hisabori, T. (2000) *J. Biol. Chem.* **275,** 35746–35750
19. Tsunoda, S. P., Rodgers, A. J., Aggeler, R., Wilce, M. C., Yoshida, M., and Capaldi, R. A. (2001) *Proc. Natl. Acad. Sci. U.S.A.* **98,** 6560–6564
20. Suzuki, T., Murakami, T., Iino, R., Suzuki, J., Ono, S., Shirakihara, Y., and Yoshida, M. (2003) *J. Biol. Chem.* **278,** 46840–46846
21. Iino, R., Murakami, T., Iizuka, S., Kato-Yamada, Y., Suzuki, T., and Yoshida, M. (2005) *J. Biol. Chem.* **280,** 40130–40134
22. Saita, E., Iino, R., Suzuki, T., Feniouk, B. A., Kinosita, K., Jr., and Yoshida, M. (2010) *J. Biol. Chem.* **285,** 11411–11417
23. Kato-Yamada, Y., and Yoshida, M. (2003) *J. Biol. Chem.* **278,** 36013–36016
24. Yagi, H., Kajiwara, N., Tanaka, H., Tsukihara, T., Kato-Yamada, Y., Yoshida, M., and Akutsu, H. (2007) *Proc. Natl. Acad. Sci. U.S.A.* **104,** 11233–11238
25. Feniouk, B. A., Kato-Yamada, Y., Yoshida, M., and Suzuki, T. (2010) *Biophys. J.* **98,** 434–442
26. Neidhardt, F. C. (1987) in *Escherichia coli and Salmonella typhimurium: Cellular and Molecular Biology*, 1st Ed., pp. 445–73, American Society for Microbiology, Washington, D. C.
27. Feniouk, B. A., Suzuki, T., and Yoshida, M. (2007) *J. Biol. Chem.* **282,** 764–772
28. Cipriano, D. J., and Dunn, S. D. (2006) *J. Biol. Chem.* **281,** 501–507
29. Konno, H., Suzuki, T., Bald, D., Yoshida, M., and Hisabori, T. (2004) *Biochem. Biophys. Res. Commun.* **318,** 17–24
30. Masaike, T., Suzuki, T., Tsunoda, S. P., Konno, H., and Yoshida, M. (2006) *Biochem. Biophys. Res. Commun.* **342,** 800–807
31. Suzuki, T., Ueno, H., Mitome, N., Suzuki, J., and Yoshida, M. (2002) *J. Biol. Chem.* **277,** 13281–13285
32. Suzuki, T., Ozaki, Y., Sone, N., Feniouk, B. A., and Yoshida, M. (2007) *Proc. Natl. Acad. Sci. U.S.A.* **104,** 20776–20781
33. Sone, N., Yoshida, M., Hirata, H., and Kagawa, Y. (1975) *J. Biol. Chem.* **250,** 7917–7923
34. Noji, H., Bald, D., Yasuda, R., Itoh, H., Yoshida, M., and Kinosita, K., Jr. (2001) *J. Biol. Chem.* **276,** 25480–25486
35. García, J. J., Ogilvie, I., Robinson, B. H., and Capaldi, R. A. (2000) *J. Biol. Chem.* **275,** 11075–11081
36. Penefsky, H. S. (1974) *J. Biol. Chem.* **249,** 3579–3585
37. Bagnara, A. S., and Finch, L. R. (1973) *Eur. J. Biochem.* **36,** 422–427
38. Morikawa, M., Izui, K., Taguchi, M., and Katsuki, H. (1980) *J. Biochem.* **87,** 441–449

[3] T. Suzuki, C. Wakabayashi, K. Tanaka, B. A. Feniouk, and M. Yoshida, unpublished observations.